Journal of Cellular Biochemistry 98:567–576 (2006)

Plugs in Nuclear Pores: Transcripts in Early Oocyte Development Identified With Nanotechniques

Andrea Schlune, Victor Shahin, Karoline Enss, Herman Schillers, and Hans Oberleithner*

Institute of Physiology II, University of Münster, Münster, Germany

Abstract Throughout oogenesis, huge amounts of RNA are produced that are needed for early development. Early stages of oocyte development are characterized by high transcriptional activity whereas translation of maternal RNA dominates late stages. Nuclear pore complexes (NPCs), located in the nuclear envelope (NE), mediate bidirectional macromolecule exchange between the nuclear and cytosolic compartments including RNA export. Here, we report on structural correlates of this transport pathway at single NPC level. Using atomic force microscopy (AFM), we imaged the nucleoplasmic (''inner'') surface of the NE of *Xenopus laevis* oocytes in different stages of development. We found that NPC frequency per nucleus increases with maturation. However, individual NPCs are more active in immature stages. In early stages, known for high transcriptional activity, we found nearly 10% of NPC central channels plugged with a 400–800 kDa mass. In contrast, the incidence of plugged NPCs was below 1% in late oocyte stages. On-site RNA digestion led to a change in plug shape from prominent to flat while plug mass decreased by almost 20%. Quantitative AFM analysis revealed that RNase exposure reduced total nucleoplasmic NPC mass by about 58 and 25% in early and late stage oocytes, respectively. We conclude: (i) NPCs of immature oocytes are more active in RNA transport, (ii) Plugs identified at the nucleoplasmic entrance of NPC central channels represent ribonucleoproteins exiting the nucleus, (iii) RNA is a structural component of the NPC nanomachine. J. Cell. Biochem. 98: 567–576, 2006.

Key words: nuclear pore complex; RNA export; nuclear envelope; oogenesis; cell nucleus

The mature anuran oocyte is an enormous cell with an informational program for embryogenesis stored in the cytoplasm. Throughout oogenesis, frog oocytes produce huge amounts of RNA, which remain dormant until fertilization. During the 6–8 months of oogenesis, the developing oocyte bears transcripts for all the proteins needed to initiate and maintain metabolism for further development. Over this time period, the maturing oocyte builds up a huge store of gene products such as mRNAs, tRNAs, structural RNAs, and proteins. Hence, high transcriptional activity is characteristic for early stages of development, during which all the rRNAs and tRNAs needed for protein synthesis until the mid-blastula stage are made and all the maternal mRNAs needed for early development are transcribed. In contrast, oocytes in late stages of development are low in transcriptional activity [Davidson et al., 1964; Golden et al., 1980; Newport and Kirschner, 1982].

The nuclear envelope (NE), a double lipid bilayer, separates the sites of transcription and translation. Nuclear pore complexes (NPCs) penetrate the NE and functionally connect the cell nucleus with the cytoplasm. Each NPC is a huge supramolecular transport machine consisting of hundreds of proteins (called nucleoporins) with an estimated total mass of ~125 MDa [Reichelt et al., 1990]. Its outstanding feature is a large central channel, variable in width, and framed by a cytoplasmic and a nucleoplasmic ring [Hinshaw et al., 1992]. A basket-like structure, which participates in messenger ribonucleoprotein (mRNP) export [Kiseleva et al., 1996], extends from the nucleoplasmic ring into the nucleoplasm. Export of RNA takes place through the NPC's large central channel [Gorlich and Mattaj, 1996; Nakielny and Dreyfuss, 1997; Cullen, 2003; Weis, 2003].

Grant sponsor: EU grant Tips4cells, Deutsche Forschungsgemeinschaft; Grant numbers: SFB 629 (A6), Re1284/2-1.

*Correspondence to: Hans Oberleithner, Institut für Physiologie II, Robert-Koch-Str. 27b, 48149 Münster, Germany. E-mail: oberlei@uni-muenster.de

Received 17 September 2005; Accepted 1 November 2005

DOI 10.1002/jcb.20742

RNA is transported as ribonucleoprotein complexes (RNPs) targeted for transport by nuclear export signals. RNA export is an active and energy-dependent process. It is class-specific [Jarmolowski et al., 1994] and mediated by signal and transport proteins [Gerace, 1995; Izaurralde and Mattaj, 1995]. The process of RNP translocation has been visualized by electron microscopy (EM) [Pante et al., 1997; Kiseleva et al., 1998]. During transport, RNPs plug the central channels of individual NPCs, as shown by a combination of atomic force microscopy (AFM) and electrical techniques [Schafer et al., 2002].

AFM developed almost 20 years ago [Binnig et al., 1986] is a suitable tool for imaging the NE surface and studying single NPC conformation [Stoffler et al., 1999; Wang and Clapham, 1999; Moore-Nichols et al., 2002; Shahin et al., 2005a,b]. Virtually all research groups using the *Xenopus laevis* nucleus as a model system for nucleocytoplasmic transport worked with late stage oocytes. They are large and easy to handle. Here, we present for the first time AFM experiments on the much smaller nuclei of early stage oocytes. Since early stage nuclei differ from late ones in terms of transcriptional activity and thus RNA export dynamics, we searched for specific structural indications at the single NPC level. We found RNA-related plugs at a 13 times higher frequency in "immature" early stage oocytes than in "mature" late stage oocytes.

METHODS

Nuclear Envelope Preparation

Female *Xenopus laevis* were anesthetized in 0.1% ethyl *m*-aminobenzoate methane sulfonate (Serva, Heidelberg, Germany) and portions of their ovaries removed. Oocytes were dissected from ovary clusters and stored in modified Ringer solution (87mM NaCl, 3mM KCl, 1mM $MgCl_2$, 1.5mM $CaCl_2$, 10mM HEPES, 100 U/100 μg penicillin/streptomycin, pH 7.4) before use.

Oocyte development can be classified into six different stages [Dumont, 1972]. This classification is largely based on the size of individual oocytes, the smallest and "youngest" ones designated as stage I, and the largest and most mature ones as stage VI. The peak of RNA synthesis occurs in stages II and III [Davidson et al., 1964; Golden et al., 1980]. As oogenesis in *Xenopus laevis* is an asynchronous process, oocytes in all stages of development are present in the ovaries of adult animals at any time. For our experiments, we compared oocytes from stage II (which will later on be referred to as "early stage") with oocytes from stage VI (which will be referred to as "late stage"). Selection of individual oocytes and allocation to the different stages of development was based on distinct morphological features according to Dumont [Dumont, 1972]: Stage II oocytes range from 350–450 μm in diameter and are of white and opaque color. Stage VI oocytes reach a diameter of more than 1,200 μm. Characteristic of this final stage of development is the appearance of a relatively unpigmented equatorial band between the animal and vegetal hemisphere.

For isolation of the nuclei, oocytes were carefully selected according to the characteristic features mentioned above and transferred into nuclear isolation medium (NIM; 90 mM KCl, 10 mM NaCl, 2 mM $MgCl_2$, 10 mM HEPES, 0.09 mM $CaCl_2$, 1.1 mM EGTA [chelates calcium to a free Ca^{2+} concentration of 10^{-8}M], pH 7.3). Nuclei were then manually isolated by piercing the oocyte with two pincers. Nuclear swelling, which occurs instantaneously when nuclei are transferred to a medium lacking macromolecules, can be prevented by adding polyvinylpyrrolidone (PVP) to the NIM. This was shown in a different series of experiments, where nuclei were isolated in NIM either in presence or in absence of 1.5% PVP ($M_r = 40{,}000$; Sigma) [Danker et al., 2001]. Nuclei were kept in NIM containing no PVP for 30 min before further preparation of the NE for AFM experiments in order to induce nuclear swelling and to unfold the NE. Then, intact nuclei were picked up with a Pasteur pipette and transferred to a glass coverslip placed under a stereomicroscope. The chromatin was carefully removed using sharp needles and the NE was spread on Cell-tak® (BD Biosciences, Bedford, MA) coated glass, with the cytoplasmic side facing downwards. Finally, the specimen were rinsed with de-ionized water and air-dried. All procedures were performed at room temperature (~23°C). NE were in an inactive state during scanning, that is, NPC transport was absent due to the experimental conditions.

Nuclear Surface Area Determination

Diameters of nuclei were measured by using light microscopy 60 min after isolation in NIM

containing no PVP. NE surface was calculated assuming that the nuclei were perfect spheres.

Atomic Force Microscopy (AFM)

The application of AFM on *Xenopus laevis* oocyte nuclei has been described in detail previously [Rakowska et al., 1998]. In short, we used a BioScope™ (NanoScope III, Digital Instruments, Santa Barbara, CA) equipped with an inverted optical microscope (Axiovert 135, Zeiss, Jena, Germany). The nucleoplasmic ("inner") NE surface was scanned with conventional V-shaped 200-μm long silicon nitride cantilevers with spring constants of 0.06 N/m and pyramidal tips with an estimated tip diameter of 10 nm (Digital Instruments). Images were recorded with 512 lines per screen applying the contact mode with a scan rate of 2–10 Hz at constant force (height mode). The forces applied during the scanning procedure were minimized by retracting the AFM-tip until it lost contact with the sample surface and re-engaging the tip at a set point (i.e., force value) minimally above the lift-off value. Scanning at such low forces left no visible marks on the NE surface. NE surface topography was analyzed by using appropriate software supplied by the manufacturer (Digital Instruments).

On-Site RNA Digestion

RNase A is an enzyme that catalyses depolymerization of single-stranded RNA. To examine the effect of RNase A on pores and plugs in a paired experimental approach, samples were first scanned before RNase A treatment and then brought into NIM plus 0.02 mg RNase A per ml for 2 h (ribonuclease A from bovine pancreas; 70 Kunitz U/mg lyophilic [Serva, Heidelberg, Germany]). For control experiments, samples were incubated in NIM for 2 h. After incubation, samples were washed in deionized water and air-dried before further AFM scanning. Identical NE areas could be scanned before and after treatment. Thus, individual pores could be compared before and after RNase treatment (Fig. 1).

Analysis of Plug Size

The plug size was measured in profile sections of the AFM images using the BioScope™ analysis software. For calculation of the plug volume (mass), the plugs were treated as perfect half-ellipsoids. In each case, the two largest diameters standing perpendicularly to each other were determined. Plug height was calculated as the vertical difference between the rim of the NPC and the top of the plug. AFM generally overestimates the diameter of biological samples due to the geometry of the tip, which induces broadening effects in the image. As a consequence, plug volume is rather overestimated in this study. From the respective molecular plug volumes (V_p, in nm^3), molecular masses (M_0, in kDa) were calculated according to the equation [Schneider et al., 1998]: $M_0 = (V_p \cdot N_0)/(V_1 + dV_2)$. Here, M_0 is the molecular mass, N_0 is Avogadro's number, and V_1 and V_2 are the partial specific volumes of the plug (0.74 cm^3/g and 1 cm^3/g water, respectively). d is the extent of plug hydration (0.4 mol H_2O/mol plug). In these calculations, the plug is treated as a pure protein, which is a simplification since the plug is a ribonucleoprotein. Using this calculation, 1 nm^3 of plug volume matches a plug mass of about 0.6 kDa. Comparison of plug volume (mass) before and after exposure to RNase A can be used to quantify the effect of RNase A on individual plugs.

Analysis of Nucleoplasmic NPC Volume

Volume of the NPC portion extending towards the nucleoplasm was analyzed using the "bearing analysis" tool of the manufacturer's software (Digital Instruments). This tool allows determining the number of voxels of a given area scanned by AFM. In our experiments, only the nucleoplasmic NPC ring structure is accessible to the AFM scanning tip and thus taken for volume analysis (termed "nucleoplasmic NPC volume"). Experiments were performed in paired manner (i.e., identical NPCs studied before and after application of RNase A), so that volumes (masses) of individual nucleoplasmic NPC ring structures could be directly compared.

Statistics

Data are shown as mean value ± standard error of the mean (SEM). In all experiments where n is not declared differently, it refers to the number of individual oocyte nuclei studied. Usually, two areas of 16 μm^2 per nucleus were used for analysis of NPC density and percentage of plugged NPCs. Significance of differences was evaluated by paired and unpaired Student's *t*-test or Mann–Whitney rank sum test, as appropriate. Significantly different is denoted by $P = 0.05$ or less and is indicated by an asterisk (*) in the graphs.

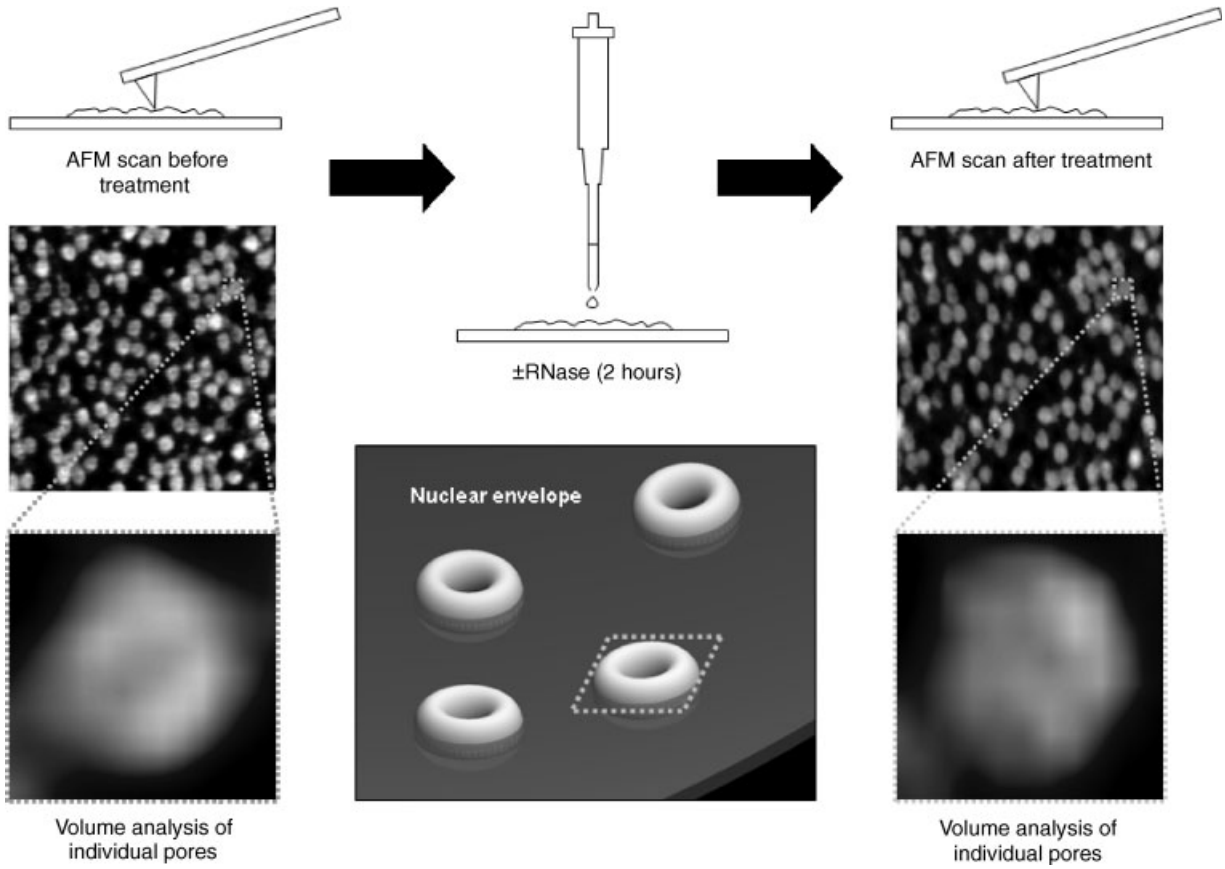

Fig. 1. On-site RNA digestion procedure. The nucleoplasmic side of a NE is scanned by AFM before and 2 h after incubation in RNase A or solvent (control). Only the nucleoplasmic ring-like structure (schematic in center) of the NPC accessible to the AFM tip on the nucleoplasmic side of the NE is used for volume analysis (zoom box = 200 nm).

RESULTS

NE Surface Area in Early and Late Stage Oocyte Nuclei

As soon as the nucleus is transferred from its natural environment, the cytosol, into NIM lacking colloid-osmotic (oncotic) pressure, salt and water move into the nucleoplasm. As the nucleus swells, the NE, usually folded in situ [Kemp, 1956], unfolds. As previously shown, 40 kDa PVP can be used to compensate for the lack of macromolecules in the NIM and to prevent nuclear swelling [Danker et al., 2001]. Figure 2 summarizes the differences in nuclear diameters at distinct stages of oocyte development in presence and absence of 1.5% PVP in NIM. In presence of PVP, nuclei maintain their original shape and volume. When stage II nuclei are transferred to NIM containing no PVP, the diameter of early stage oocyte nuclei increases by $7 \pm 2.9\%$ ($n = 5$). In stage VI oocytes, the increase of nuclear diameter in absence of macromolecules is much more prominent. Here, the nuclear diameter increases by $60 \pm 5.8\%$ ($n = 9$). Consequently, a careful distinction must be made between the "apparent" (folded) NE surface area and the "true" (unfolded) NE surface area, which is derived from the diameter of the swollen nucleus in absence of PVP. The "true" NE surface area is 0.28 ± 0.029 mm^2 ($n = 5$) in early stage nuclei and 1.99 ± 0.125 mm^2 ($n = 9$) in late developmental stages. Taken together, the NE surface is more than seven times larger in late stage oocyte nuclei than in early stage oocyte nuclei. These large differences between "apparent" (folded) and "true" (unfolded) NE surface area must be taken into account when total numbers of NPCs per nucleus are calculated.

NPC Density in Early and Late Stage Oocyte Nuclei

Figure 3 shows the nucleoplasmic NE surface of early and late stage oocytes as seen by AFM.

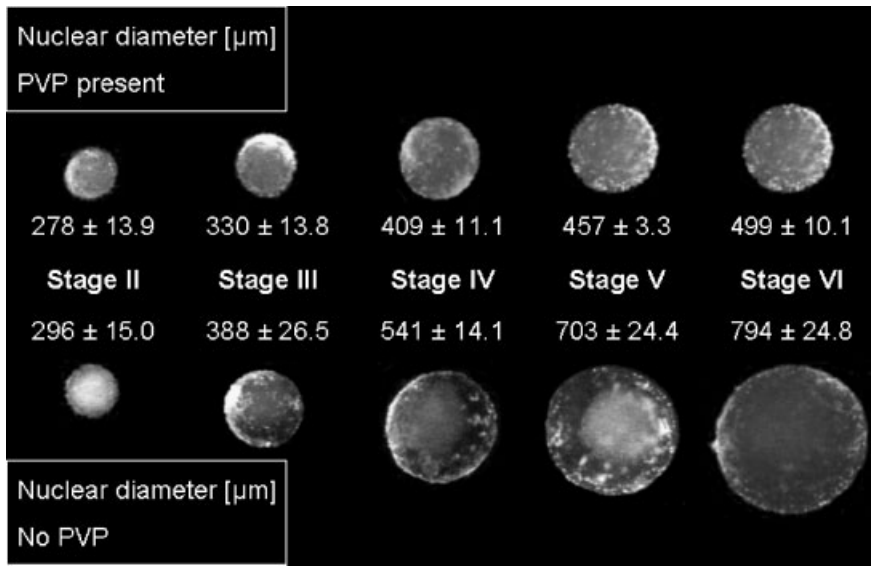

Fig. 2. Nuclear diameters at different stages of oocyte development in presence and absence of polyvinylpyrrolidone (PVP) in nuclear isolation medium. In presence of PVP nuclei maintain their original volume whereas a substantial volume increase is observed in absence of PVP. Displayed nuclei are matched pairs (i.e., one and the same nuclei before and after swelling).

In early stages II, NPC density (31.6 ± 1.67 NPCs/μm^2; $n = 34$, number of NE areas studied) is significantly higher as compared to late stages VI (23.4 ± 1.07 NPCs/μm^2; $n = 29$; $P < 0.001$).

The total number of NPCs per oocyte nucleus can be calculated from the given data of NE surface area and NPC density. In early stage oocytes, the total number of NPCs per nucleus is $8.8 \pm 0.24 \cdot 10^6$ compared to $46.8 \pm 0.88 \cdot 10^6$ NPCs present in late stage nuclei (Fig. 4). Thus, the total number of NPCs per oocyte in late stages of development is more than five times higher as compared to early stages.

NPC Plugs

A certain percentage of NPCs contains large masses occluding their central channels. We call such macromolecules located in the NPC centers, "plugs." Plugs probably represent ribonucleoproteins (RNPs) exported by the NPCs [Schafer et al., 2002; Oberleithner et al., 2003]. The percentage of plugged NPCs is $9.2 \pm 1.73\%$ ($n = 18$, number of NE areas studied) in early stage oocyte nuclei and only $0.7 \pm 0.43\%$ ($n = 7$) in late stages. Hence, transcriptionally active oocytes display a more than 13 times higher percentage of plugged NPCs than do transcriptionally less active oocytes. In other words, in early stage oocytes $807{,}858 \pm 13{,}138$ NPCs per nucleus are plugged compared to $60{,}847 \pm 2{,}900$ plugged NPCs per nucleus in late developmental stages. Although the total number of NPCs per nucleus is lower in early than in late oocyte stages, the number of plugged NPCs in early stages of development significantly exceeds the one found in late stages ($P < 0.001$) as displayed in Figure 4A,B.

Since plugs in the NPC central channels most likely represent ribonucleoproteins exported by the NPCs, a change in shape upon exposure to RNase A was postulated. As displayed in two representative examples in Figure 5, plug shape changes upon exposure to RNase A. Plug height decreases while plugs broaden. From the three-dimensional images, we calculated plug volume (mass) before and after incubation in RNase A solution. Volume analysis of nine plugs before and after incubation in RNase A solution indicates a significant decrease in plug volume (mass) to $82.3 \pm 4.98\%$ of the original size ($P = 0.03$).

Nucleoplasmic NPC Volume

We observed that not only plugs located in the NPC central channels shrink upon exposure to RNase A but also the total nucleoplasmic NPC ring structure (Fig. 6). RNase A treatment induces significant reductions in nucleoplasmic NPC volume from initial ($100\% = \text{control}$) values to $42.5 \pm 5.19\%$ in early stage and to $74.7 \pm 4.15\%$ in late stage oocytes. In contrast,

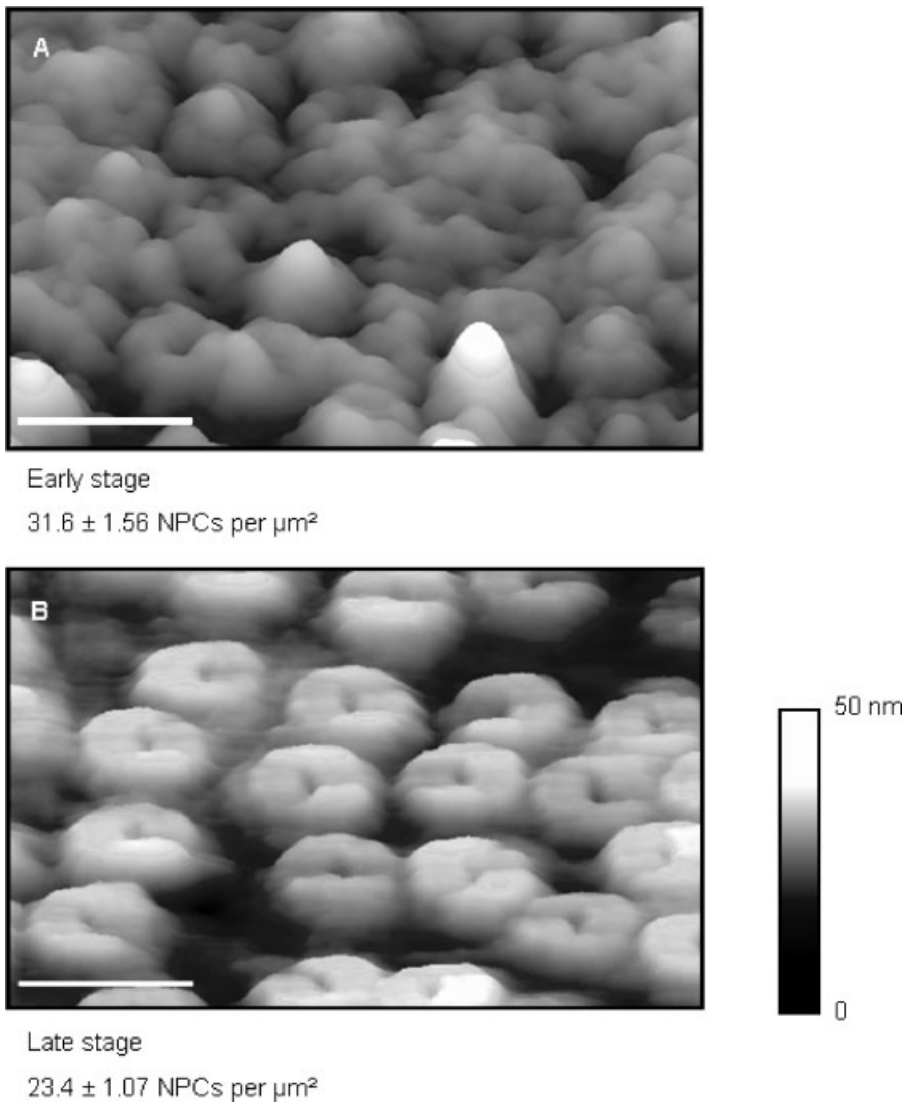

Fig. 3. AFM images of the NE nucleoplasmic surface in early (**A**) and late (**B**) stages of oocyte development (scale bar = 250 nm). In early stages II, some NPCs are plugged and NPC density is higher than in late stages VI.

NPCs exposed to medium lacking RNase A for 2 h (control) rather increase in size. Taken together, the nucleoplasmic NPC ring structure shrinks in response to RNase A treatment significantly more in early than in late stage oocytes.

DISCUSSION

NEs of different stages of oocyte development have not yet been investigated with AFM. This seemed desirable since an individual oocyte undergoes a dramatic change in structure and function when it develops from the early immature stage to the late mature stage. Such macroscopic changes should by reflected at single NPC level.

Quantitative Aspects of Nuclear Pore Density in Early and Late Stages

In the present study, we found a nuclear pore density of 31.6 ± 1.67 NPCs/μm^2 in early stages and of 23.4 ± 1.07 NPCs/μm^2 in late stages. In contrast, investigations carried out in the 1970s with negative staining methods and EM led to substantially higher values for NPC density, namely 63.0 ± 4.4 NPCs/μm^2 for early stage oocytes and 47.0 ± 3.3 NPCs/μm^2 for late stage

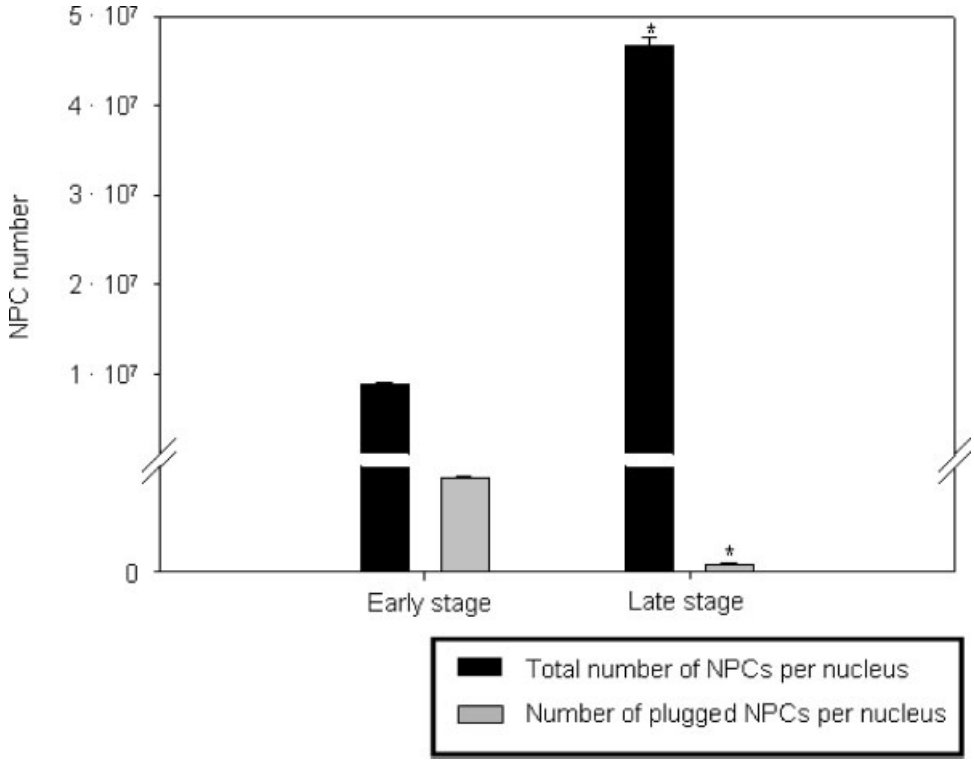

Fig. 4. Comparison of the total number of NPCs and the number of plugged NPCs per nucleus in early (stage II) and late developmental stages (stage VI). Asterisks (*) indicate a statistically significant difference between early and late stage ($P < 0.001$).

oocytes [Scheer, 1973]. This apparent discrepancy is most likely due to technical reasons [Speth and Wunderlich, 1970]. In fact, the fragments used for the EM studies may not be representative for the whole NE. Negative staining leads to the selection of those NE fragments that have the highest pore frequency because during NE isolation and grid attachment the fragments with the highest pore frequency tend to stick together [Maul, 1977]. AFM preparations use native NEs and thus avoid this problem. Selection of flat membrane areas used for the AFM assessment of NPC density is virtually random.

"True" Nuclear Surface Is Important to Quantify Pores per Nucleus

Calculation of total number of NPCs per cell nucleus is based on nuclear pore density and nuclear surface area. Considering the relatively small difference in NPC density (factor of 1.4, early/late stages) compared to the massive difference in NE surface area (factor of 7.2, early/late stages), it is evident that the nuclear surface area is the major variable during oocyte development. In this context, it is of paramount importance to calculate total NPC number per nucleus on the basis of "true" NE surface area gained from volume-expanded nuclei. We calculated a total NPC number of $8.8 \pm 0.02 \cdot 10^6$ per nucleus for early oocyte stages and of $46.8 \pm 0.88 \cdot 10^6$ per nucleus for late oocyte stages. On the basis of EM investigations, the total number of pores per nucleus was calculated to be $14.4 \cdot 10^6$ for early stages and $37.7 \cdot 10^6$ for late stages of development [Scheer, 1973]. We think that the present AFM data are more close to reality because EM staining causes overestimations of NPC density (see paragraph above) while lack of swelling (see above) underestimates the true nuclear surface area. This could explain the high values in early stage and the low values in late stage oocyte nuclei of the EM studies.

High NPC numbers do not necessarily indicate substantial nucleocytoplasmic RNA transport. In fact, late stage oocytes have considerably more nuclear pores as early stage oocytes due to the much larger surface area of the former. In contrast, NPCs of early stage

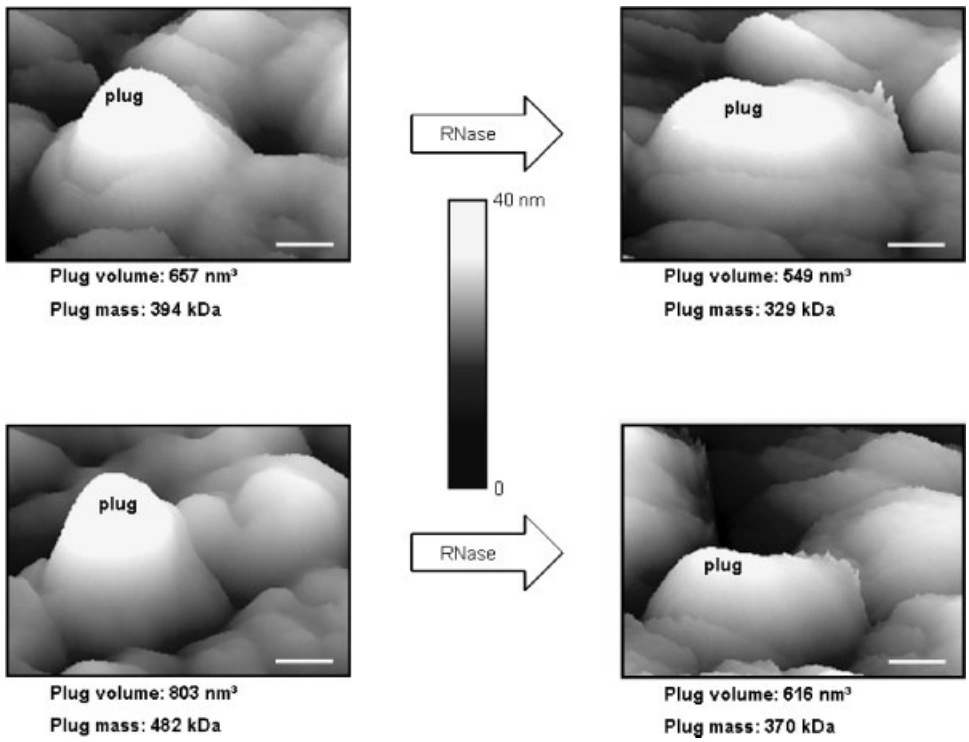

Fig. 5. AFM plug analysis before and after 2 h after incubation with RNase A. Two typical examples of individual plugs before and after exposure to RNase A are given (matched pairs). A decrease in plug height and an increase in plug width can be observed (scale bar = 50 nm).

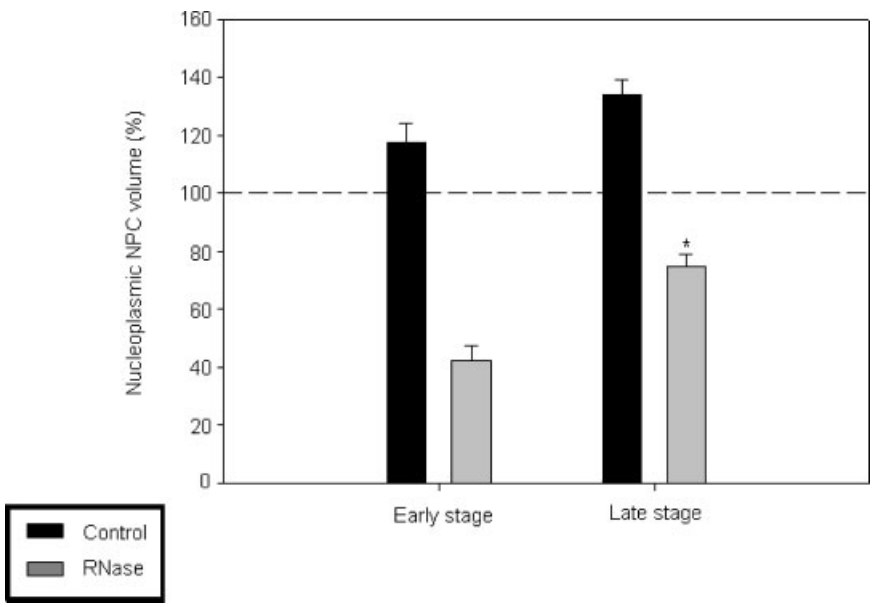

Fig. 6. Nucleoplasmic NPC volume change upon treatment with RNase A in early and late stages of development. Mean data ± SEM are given; n = 15 (number of individual NPCs studied). A significant decrease in nucleoplasmic NPC volume in response to RNase A incubation is observed in both early ($P < 0.001$) and late ($P < 0.001$) stages of oocyte development. The asterisk (*) indicates a significant difference ($P < 0.001$) in volume change between early and late developmental stages. Controls show a significant increase in nucleoplasmic NPC volume upon incubation in NIM in early ($P = 0.05$) and late ($P < 0.001$) developmental stages but no significant difference between different stages.

oocytes are more active indicated by a 13 times higher number of plugged NPCs, a correlate for transcriptional activity (see below).

Nucleoplasmic Plugs in Pores

Plugs are large masses (400–800 kDa) that completely occupy the nucleoplasmic channel entrance. They are easily detectable by AFM. However, as the NPC central channel is approximately 50 nm in length and only a few nm wide in its middle, it is not completely accessible to the AFM scanning tip. As a consequence, plugs concealed in the depth of the NPC cannot be detected by the AFM tip. Thus, plug frequency in both early and late stages of development is rather underestimated.

There identity of plugs is still under discussion [Akey, 1990; Jarnik and Aebi, 1991; Schwartz, 2005]. Plugs are sometimes considered as preparation artifacts caused by, for example, the nuclear basket collapsing into the NPC lumen during fixation. Since we work with native Nes, this view can be ruled out. In addition, it is unlikely that such artifacts would occur 13 times more frequently in early stages than in late ones. Furthermore, there is evidence that a centrally located plug is an intrinsic part of the NPC transport machine. Finally, the plug could be a cargo molecule (complex) caught in transit through the NPC.

Plugs Are RNPs Identified by On-Site RNase Digestion

In a previous study, it was shown that a single injection of a *Xenopus laevis* oocyte with a steroid hormone provokes plug formation 20 min later [Schafer et al., 2002]. Plug appearance is paralleled by a sharp increase in electrical NE resistance. Since the transcription inhibitor actinomycin D or RNase A incubation eliminated the resistance increase, the conclusion was made that RNP export through the NPC could be the underlying mechanism [Schafer et al., 2002; Oberleithner et al., 2003]. The present article supports this view. Plugs change in shape and decrease in molecular mass by about 18% upon a 2-h treatment with RNase A. This suggests that plugs consist, at least partially, of RNA. The major portion of the plug most likely consists of proteins. Obviously, plugs are the morphological correlate of RNPs.

As elegantly shown by high-resolution scanning, EM RNPs first bind to the NPC basket before translocation occurs [Kiseleva et al., 1998]. In the preparation, we use the baskets that have been most likely removed by the isolation procedure. Therefore, we detect plugs only when already tightly anchored inside the dilated central channel. A large number of proteins with specific functions participates in RNA export. Receptor and adaptor proteins are loaded cotranscriptionally to nascent RNAs to form large RNP complexes [Stutz and Izaurralde, 2003]. The RNP complex is first oriented in a specific manner at the pore entrance followed by RNA unpacking and translocation [Mehlin et al., 1992]. Since the resolution of our AFM images is limited so that we cannot distinguish individual proteins of the NPC machine, we measured the total volume (mass) of the NPC ring structure that protudes from the nucleoplasmic surface. We assumed that even in absence of a visible plug, RNA could be "hidden" inside the ring-like structure. With on-site RNase treatment, we could perform paired experiments and quantify the NPC mass before and after exposure. The results indicate that RNA is present in the NPC machinery. Consistent with plug frequency, RNA is more abundant in NPCs of early stage oocytes.

In summary, the data indicate that the plugs located in the NPC central channel are a visible morphological correlate for the transcriptional activity of the cell. In early stage oocytes, plugged NPCs are frequently found, while in late stages of oocyte development, plugging is rare unless induced exogenously by the application of hormones [Schafer et al., 2002]. On-site digestion studies indicate that RNA is a structural component of NPCs.

ACKNOWLEDGMENTS

We thank Marianne Wilhelmi for excellent technical assistance and Ingrid Winkelhues for great help in statistical analysis of the data. Work in the senior author's laboratory was performed by A.S. in the fulfillment of the thesis requirements for the Medical Degree (MD).

REFERENCES

Akey CW. 1990. Visualization of transport-related configurations of the nuclear pore transporter. Biophys J 58:341–355.

Binnig G, Quate CF, Gerber C. 1986. Atomic force microscope. Phys Rev Lett 56:930–933.

Cullen BR. 2003. Nuclear RNA export. J Cell Sci 116:587–597.

Danker T, Shahin V, Schlune A, Schafer C, Oberleithner H. 2001. Electrophoretic plugging of nuclear pores by using the nuclear hourglass technique. J Membr Biol 184:91–99.

Davidson EH, Allfrey VG, Mirsky AE. 1964. On the RNA synthesized during the lampbrush phase of amphibian oogenesis. Proc Natl Acad Sci USA 52:501–508.

Dumont JN. 1972. Oogenesis in *Xenopus laevis* (Daudin). I. Stages of oocyte development in laboratory maintained animals. J Morphol 136:153–179.

Gerace L. 1995. Nuclear export signals and the fast track to the cytoplasm. Cell 82:341–344.

Golden L, Schafer U, Rosbash M. 1980. Accumulation of individual pA+ RNAs during oogenesis of *Xenopus laevis*. Cell 22:835–844.

Gorlich D, Mattaj IW. 1996. Nucleocytoplasmic transport. Science 271:1513–1518.

Hinshaw JE, Carragher BO, Milligan RA. 1992. Architecture and design of the nuclear pore complex. Cell 69: 1133–1141.

Izaurralde E, Mattaj IW. 1995. RNA export. Cell 81:153–159.

Jarmolowski A, Boelens WC, Izaurralde E, Mattaj IW. 1994. Nuclear export of different classes of RNA is mediated by specific factors. J Cell Biol 124:627–635.

Jarnik M, Aebi U. 1991. Toward a more complete 3-D structure of the nuclear pore complex. J Struct Biol 107: 291–308.

Kemp NE. 1956. Differentiation of the cortical cytoplasm and inclusions in oocytes of the frog. J Biophys Biochem Cytol 2:187–190.

Kiseleva E, Goldberg MW, Daneholt B, Allen TD. 1996. RNP export is mediated by structural reorganization of the nuclear pore basket. J Mol Biol 260:304–311.

Kiseleva E, Goldberg MW, Allen TD, Akey CW. 1998. Active nuclear pore complexes in Chironomus: Visualization of transporter configurations related to mRNP export. J Cell Sci 111(Pt 2):223–236.

Maul GG. 1977. The nuclear and the cytoplasmic pore complex: Structure, dynamics, distribution, and evolution. Int Rev Cytol Suppl 6:75–186.

Mehlin H, Daneholt B, Skoglund U. 1992. Translocation of a specific premessenger ribonucleoprotein particle through the nuclear pore studied with electron microscope tomography. Cell 69:605–613.

Moore-Nichols D, Arnott A, Dunn RC. 2002. Regulation of nuclear pore complex conformation by IP(3) receptor activation. Biophys J 83:1421–1428.

Nakielny S, Dreyfuss G. 1997. Nuclear export of proteins and RNAs. Curr Opin Cell Biol 9:420–429.

Newport J, Kirschner M. 1982. A major developmental transition in early *Xenopus* embryos: II. Control of the onset of transcription. Cell 30:687–696.

Oberleithner H, Schafer C, Shahin V, Albermann L. 2003. Route of steroid-activated macromolecules through nuclear pores imaged with atomic force microscopy. Biochem Soc Trans 31:71–75.

Pante N, Jarmolowski A, Izaurralde E, Sauder U, Baschong W, Mattaj IW. 1997. Visualizing nuclear export of different classes of RNA by electron microscopy. RNA 3: 498–513.

Rakowska A, Danker T, Schneider SW, Oberleithner H. 1998. ATP-Induced shape change of nuclear pores visualized with the atomic force microscope. J Membr Biol 163:129–136.

Reichelt R, Holzenburg A, Buhle EL, Jr., Jarnik M, Engel A, Aebi U. 1990. Correlation between structure and mass distribution of the nuclear pore complex and of distinct pore complex components. J Cell Biol 110:883–894.

Schafer C, Shahin V, Albermann L, Hug MJ, Reinhardt J, Schillers H, Schneider SW, Oberleithner H. 2002. Aldosterone signaling pathway across the nuclear envelope. Proc Natl Acad Sci USA 99:7154–7159.

Scheer U. 1973. Nuclear pore flow rate of ribosomal RNA and chain growth rate of its precursor during oogenesis of *Xenopus laevis*. Dev Biol 30:13–28.

Schneider SW, Larmer J, Henderson RM, Oberleithner H. 1998. Molecular weights of individual proteins correlate with molecular volumes measured by atomic force microsocopy. Pflugers Arch 435:362–367.

Schwartz TU. 2005. Modularity within the architecture of the nuclear pore complex. Curr Opin Struct Biol 15:221–226.

Shahin V, Albermann L, Schillers H, Kastrup L, Schafer C, Ludwig Y, Stock C, Oberleithner H. 2005a. Steroids dilate nuclear pores imaged with atomic force microscopy. J Cell Physiol 202:591–601.

Shahin V, Ludwig Y, Schafer C, Nikova D, Oberleithner H. 2005b. Glucocorticoids remodel nuclear envelope structure and permeability. J Cell Sci 118:2881–2889.

Speth V, Wunderlich F. 1970. The macronuclear envelope of Tetrahymena pyriformis GL in different physiological states. 3. Appearance of freeze-etched nuclear pore complexes. J Cell Biol 47:772–777.

Stoffler D, Goldie KN, Feja B, Aebi U. 1999. Calcium-mediated structural changes of native nuclear pore complexes monitored by time-lapse atomic force microscopy. J Mol Biol 287:741–752.

Stutz F, Izaurralde E. 2003. The interplay of nuclear mRNP assembly, mRNA surveillance and export. Trends Cell Biol 13:319–327.

Wang H, Clapham DE. 1999. Conformational changes of the in situ nuclear pore complex. Biophys J 77:241–247.

Weis K. 2003. Regulating access to the genome: Nucleocytoplasmic transport throughout the cell cycle. Cell 112:441–451.